

# Alginate/Gauze Incorporated with *Hibiscus sabdariffa* Linn. Extract as a Bioactive Agent for Wound Dressing Application

Siti Pauliena Mohd Bohari<sup>a,b,\*</sup>, Nursyafika Az Zahra Ajan<sup>a</sup>

<sup>a</sup> Department of Biosciences, Faculty of Science, Universiti Teknologi Malaysia, 81310 Skudai, Johor Malaysia

<sup>b</sup> Institute of Bioproduct Development, Universiti Teknologi Malaysia, 81310 Skudai, Johor Malaysia

## Article history

Received

31 March 2023

Revised

18 April 2023

Accepted

18 April 2023

Published online

25 May 2023

\*Corresponding author  
pauliena@utm.my

## Abstract

In recent years, the development of wound dressings has changed from a passive to an active form by adding antiseptic agents such as polyvinylpyrrolidone (PVPi) and nanoparticles such as silver nanoparticles to facilitate the wound healing process. However, PVPi is toxic to human skin fibroblasts, and silver nanoparticles may result in metal accumulation in the tissues due to their nanosize. Therefore, a new approach to using natural sources from plants such as *Hibiscus sabdariffa* Linn. (HSL) is promising due to its phytochemical constituents that can serve as a potential therapeutic agent in wound dressings. In this study, freeze-dried alginate/gauze (FDA/gauze) without and with HS extract and calcium alginate/gauze (CA/gauze) with and without HS extract were developed by freeze-drying and gelation, respectively. This study aimed to characterize the properties of alginate/gauze-dressings as wound dressings. The morphology of the designed dressing; FDA/gauze, looks evenly distributed on the surface of the gauze compared to CA/gauze. It was found that FDA/gauze dressings have higher water absorbency than CA/gauze dressings, ranging from 690.43 to 1340.86% from day 1 until day 14. The percentage of water uptake ability increases as the concentration of alginate increases. In addition, the seeded human skin fibroblasts' growth on the alginate/gauze dressings infused with HSL extract growth in clustered, bright, and colourless proves that the cells were viable. Thus, the addition of HSL extract shows to support the process of cell viability.

**Keywords** Alginate, *Hibiscus sabdariffa* Linn, hydrogel, human dermal fibroblast

© 2023 Penerbit UTM Press. All rights reserved

## 1.0 INTRODUCTION

Disruption of skin function or integrity due to burns, injuries, or diseases is defined as a wound and is often caused by infections, genetic disorders, surgery, trauma, and abrasions (Bhardwaj et al., 2018; Kamoun et al., 2017). Wounds can be classified as acute or chronic depending on the healing time and severity of the wound (Aderibigbe & Buyana, 2018). A chronic wound takes longer to heal because it involves more tissue loss, which affects vital components like nerves and joints, and heals completely within 8 to 12 weeks with little scarring (Aderibigbe & Buyana, 2018).

A wound can naturally heal by the regrowth of the missing and damaged tissue, but an efficient wound dressing is required to speed up the healing process (Boateng and Catanzano, 2015). The application of wound dressing is important to mediate the proper phase and create favourable conditions for wound healing (Summa et al., 2018). In general, an effective wound dressing should be able to absorb wound exudates, maintain a moist environment, allow adequate gas exchange, have no toxic effects, facilitate cell migration and proliferation, and regulate the release of growth factors (Bagher et al., 2020). In addition, the wound dressing must be easily removable without traumatizing the newly formed tissue to promote wound healing (Aderibigbe and Buyana, 2018).

Based on the above requirements, a natural polymer is a promising candidate that meets all the requirements to be used as a material for wound dressings. Biopolymers are usually used due to their water absorption capacity, mechanical strength, biocompatibility, biodegradability, readily available and low cost (Summa et al., 2018).

Among the biopolymers available, alginate, derived from brown algae and composed of  $\alpha$ -L-guluronic acids (G-chain) and  $\beta$ -D-mannuronic acids (M-chain), is widely used in pharmaceutical and biomedical applications (Catanzano et al., 2015). Ionic interaction between guluronic acids and divalent cations such as  $\text{Ca}^{2+}$  ions leads to the formation of an "egg-box" structure in gel form (Aderibigbe and Buyana, 2018). This makes alginate dressings an ideal material for producing a wound dressing that can provide moisture to the wounded site (Boateng and Catanzano, 2015). Although alginate dressings can control the wound-healing process, proper and rapid wound healing is critical to prevent impaired or delayed wound healing (Summa et al., 2018).

In recent years, the design of advanced wound dressings has changed from a passive form that does not play an active role in wound healing (cotton and gauze) to an active form in which biological components are incorporated into the dressing (antibacterial agents or plant extracts) that have a specific function and play an active role in rapid wound healing (Boateng and Catanzano, 2015). Plants are used in traditional medicine to cure a variety of diseases. They are known to have less harmful effects, are naturally abundant, and are economical (Riaz & Chopra, 2018).

Extracts of roselle (*Hibiscus sabdariffa* Linn.) are known to have antibacterial properties against human pathogens and both Gram-positive and Gram-negative microorganisms (Alshami & Alharbi, 2014). The presence of flavonoids in HSL extract is attributed to their antimicrobial activity, in which they form complexes with the cell wall and cause the exit of ions from bacterial cells (Riaz & Chopra, 2018). The antibacterial property of HSL is important to protect the wound area from microbial infection during the healing process and to avoid prolonged infections that may increase the incidence of chronic wounds, leading to delayed wound healing (Summa et al., 2018). Therefore, the present work aimed to characterize the properties of alginate/gauze dressings with different alginate concentrations and preparations. Later, the survivability of human skin fibroblasts (HSF) in the alginate dressings infused with HSL extract was also observed.

## 2.0 MATERIALS AND METHODS

### 2.1 Materials

Low viscosity sodium alginate from Kelp (brown seaweed) (viscosity = 20– 40 centipoise (cp) for 2% solution at 25°C cat no: 180947, Mw = 120,000–190,000, M:G (mannuronic:guluronic) ratio 1.56–0.64) was purchased from Acros Organics (New Jersey, United States of America). Dulbecco's Modified Eagle's Medium (DMEM) High Glucose (4.5 g/L) with stable glutamine and sodium pyruvate (Cat No: DMEM-HPSTA) and Fetal Bovine Serum Advanced (FBS) (Cat No: FBS-11A) were purchased from Capricorn Scientific (Auf der Lette, Ebsdorfergrund, Germany). Antibiotic-Antimycotic (100X) from Gibco (Grand Island, New York, United States) and Phosphate Buffered Saline (PBS) tablets, pH 7.4 (Cat No: T9181) from Takara Bio Inc (Kusatsu, Shiga, Japan).

### 2.2 Hibiscus Sabdariffa Linn. (HSL) extract preparation

The HSL extract was provided by a PhD student, Mr Hafedh Ahmed, from Tissue Engineering Laboratory, Department of Biosciences, Faculty of Science, Universiti Teknologi Malaysia.

### 2.3 Preparation of alginate solution

Sodium alginate 1% and 2% (w/v) was dissolved in 100 ml of distilled water using an analytical balance and placed into a 250 ml Schott bottle. It was then stirred until it completely dissolved into a homogenizing solution. The sodium alginate solution was allowed to stand overnight to obtain a uniform solution (Mohandas et al., 2015).

#### 2.3.1 Freeze-dried alginate/gauze (FDA/gauze)

The gauze was cut into small pieces that fit the size of the 12-well plate and placed in each well. One ml of a 1% and 2% (w/v) sodium alginate solution was pipetted onto the gauze in each well and kept overnight in the refrigerator (-20°C) before being sent to the freeze dryer. Thereafter, the freeze-dried alginate and gauze were stored in the desiccator containing silica beads to control the humidity until further use (Mohandas et al., 2015).

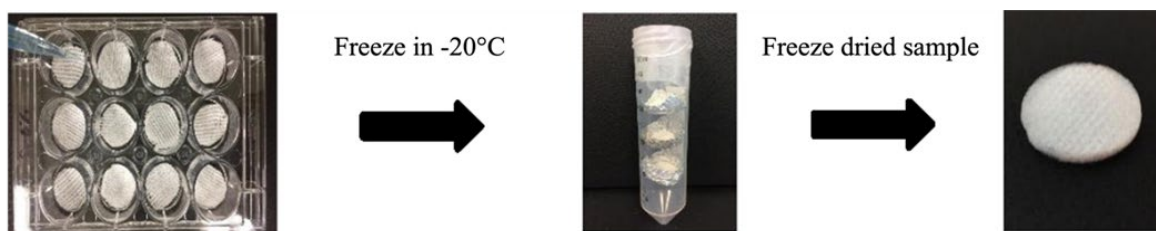


**Figure 1** Photograph representation of fabrication of Freeze-dried alginate/gauze (FDA/gauze)

### 2.3.2 Calcium alginate/gauze (CA/gauze)

The gauze was cut into small pieces that fit the size of the 12-well plate and placed in each well. One ml of a 1.0% and a 2.0% sodium alginate solution was transferred into each well over the gauze using a pipet and covered with filter paper. Later, a 100 mM calcium chloride solution was transferred onto the surface of the filter paper and allowed to stand at room temperature for 1.5 h until solidified. (Bohari et al., 2011).



**Figure 2** Photograph representation of fabrication of calcium alginate/gauze (CA/gauze)

## 2.4 Characterization of Alginate Dressings

### 2.4.1 Scanning Electron Microscopy (SEM)

Wound dressings (FDA/gauze and CA/gauze) were coated with gold for 10 minutes using a Leica EM Ace 200 vacuum coater. The morphology of the alginate/gauze dressings was examined using Hitachi Tabletop Scanning Electron Microscopy (Mohandas et al. 2015, Chen et al., 2017, Kong et al., 2019, Sobhanian et al., 2019).

### 2.4.2. Water Uptake Ability

Determination of the water absorption capacity of FDA/gauze and CA /gauze was observed by a swelling experiment. To mimic wound conditions, a solution consisting of 8.298 g sodium chloride (NaCl) and 0.368 g calcium chloride dihydrate ( $\text{CaCl}_2 \cdot 2\text{H}_2\text{O}$ ) was prepared (Lencina et al., 2015). Before the samples were immersed in the solution, their initial weight was determined and noted as  $W_d$ . Then, the samples were placed in a centrifuge tube and wound solution was pipetted into each tube. The samples were left at 37°C in a Gerhardt incubator shaker (THO500), and the two alginate/gauze dressings were removed at intervals after 1, 3, 7, 9, and 14 days of incubation and weighed, noted as  $W_w$ . All samples were prepared in triplicate in the experiment. The swelling ratio of the alginate dressings was calculated using the following formula (Mohandas et al., 2015).

$$\text{Water Uptake Ability} = [(W_w - W_d) / W_d] \times 100 \quad (\text{Equation 1})$$

## 2.5 Cell viability study

Alginate/gauze dressings (FDA/gauze and CA /gauze) were sterilized under ultraviolet (UV) light for 4 hours and placed in a 6-well plate. 17  $\mu\text{l}$  of HSL extract was added to the surface of the dressings and left for 5 minutes to allow the absorption of roselle extract into the alginate dressings. Human skin fibroblasts (HSF) at a density of  $1 \times 10^6$  cells were seeded onto the alginate dressings. 2.5 ml of complete medium was carefully added to each well and incubated at 37°C in 5% carbon dioxide. Attachment of cells to the alginate dressings was observed under Nikon Eclipse inverted microscope (TS100) after 24 hours of incubation (Mohandas et al., 2015).

## 3.0 RESULTS AND DISCUSSION

### 3.1 Characterization of alginate/gauze dressings

#### 3.1.1 Morphology study of alginate/gauze-dressings

The properties of the prepared freeze-dried alginate/gauze (FDA/gauze) and calcium alginate/gauze (CA /gauze) dressings are shown in Figure 3 below. It can be seen from the images that the FDA looks evenly distributed on the surface of the gauze compared to CA on the gauze.

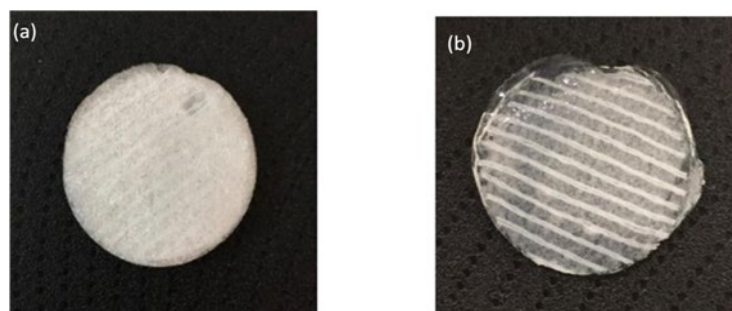


**Figure 3** Photographs of (a) Freeze-dried alginate/gauze (FDA/gauze) and (b) Calcium alginate/gauze (CA/gauze)

### 3.1.2 Scanning Electron Microscopy (SEM)

The morphology of different forms of alginate/gauze- dressings, freeze-dried alginate/gauze (FDA/gauze) and calcium alginate/gauze (CA/gauze) with different concentrations (1.0% and 2.0%) were observed using Hitachi Table Top Scanning Electron Microscopy (113145-07). Figure 4 shows the morphology of the gauze as a negative control. The strands of the gauze can be seen at 100x, 500x and 1000x magnification.

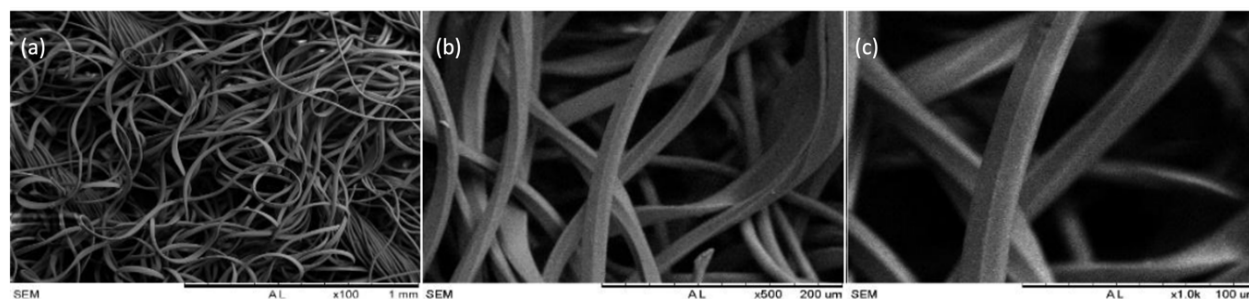


**Figure 4** SEM images of gauze as a negative control with different magnifications, (a) 100x, (b) 500x and (c) 1000x

Freeze-dried alginate/gauze (FDA/gauze) is also known as an alginate-based sponge and can be easily prepared through single-step freeze-drying (Sun & Tan, 2013). The shape of the sponge can be predicted, and the mechanical strength was highly dependent on the structural parameters such as porosity, orientation and size (Sun & Tan, 2013). Based on Figures 5a and 5c (1% FDA/gauze dressing) and Figures 5b and 5d (2% FDA/gauze dressing), the structures for both FDA/gauze dressings and FDA without gauze (control) consisted of pores with irregular sizes. According to Wan et al. (2014), they found that pure alginate had a highly porous structure in which the pores were interconnected. Saarai et al. (2012) studied that samples with pure sodium alginate had aggregated and particle-like structures. Bahadoran et al. (2020) reported that more pores are formed as the concentration of alginate increases. The observation shows that 1% FDA/gauze dressing formed more pores than 2% FDA/gauze dressing due to a lower alginate concentration. Furthermore, 1% FDA/gauze dressing also has larger pores than 2% FDA/gauze dressing. This is because a small amount of alginate provides more space for larger pores to form. In contrast, 2% FDA/gauze dressing has more alginate and more pores are formed but the space is limited which resulted in the formation of small pores. Therefore, the amount of alginate is one of the factors that contribute to the size and number of pores formed (Bahadoran et al., 2020).

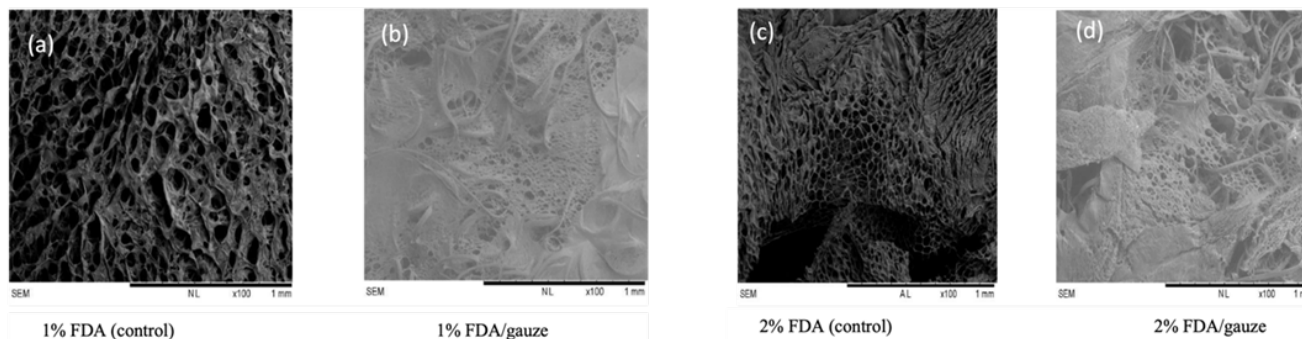


**Figure 5** SEM images of (a and c) 1 and 2% of freeze-dried alginate (FDA) as a control without gauze and (b,d) and 2% freeze-dried alginate/gauze (FDA/gauze) at different magnifications 500x



On the other hand, it was obvious that the morphology of CA/gauze dressings was different from that of FDA/gauze dressings, where the surface of CA/gauze dressings was smooth due to the binding of alginate with a crosslinker such as calcium chloride ( $\text{CaCl}_2$ ), as shown in Figure 6. The non-porous structure of CA/gauze dressings was due to the interaction of the guluronic acid blocks of alginate in the presence of divalent cations (Oh et al., 2020). In comparison, the lack of a crosslinking process in the fabrication of FDA/gauze dressings led to the formation of a highly porous structure. Among the divalent cations, alginate has a strong affinity for calcium ions ( $\text{Ca}^{2+}$ ), followed by strontium ( $\text{Sr}^{2+}$ ) and barium ions ( $\text{Ba}^{2+}$ ) (Andersen et al., 2015). The selectivity of similar alkali metals to alginate depends on the chemical distribution of the G-chains.  $\text{Ca}^{2+}$  ions can bind to both G-chains and alternating GM blocks, while  $\text{Sr}^{2+}$  ions bind tightly to G-chains but not at all to M-chains (Montanucci et al., 2015). As for  $\text{Ba}^{2+}$  ions, they can bind to separate G and M chains, but not to alternating GM chains (Montanucci et al., 2015). Ionic crosslinking between guluronic acids and  $\text{Ca}^{2+}$  ions from calcium chloride ( $\text{CaCl}_2$ ) is known to be a gelation process that occurs instantaneously and forms an 'egg-box' structure, as shown in Figure 7 (Andersen et al., 2015). Through multiple coordination, the "egg-box" structure was formed when  $\text{Ca}^{2+}$  ions bind to the oxygen atoms of the carboxyl groups ( $\text{COO}^-$ ) of the guluronic acid chains (Aderibigbe and Buyana, 2018).

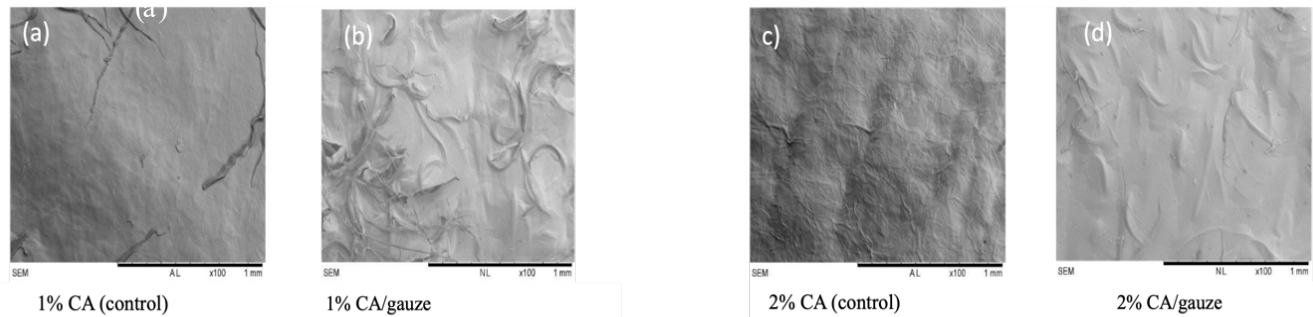


**Figure 6** SEM images of (a and c) 1 and 2% of calcium-dried alginate (FDA) as a control without gauze and (b,d) and 2% calcium-dried alginate/gauze (FDA/gauze) at different magnifications, (a and b) 100x, (c and d) 500x

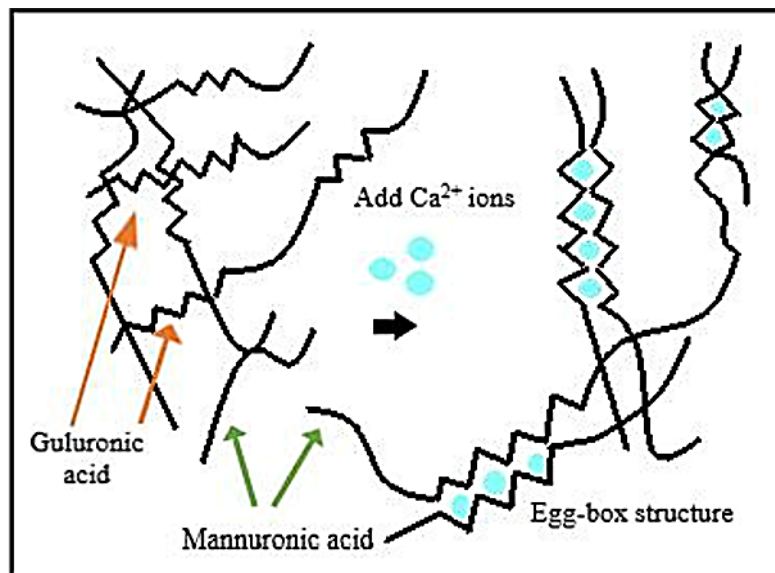


**Figure 7** Formation of "egg-box" structure of alginate with  $\text{Ca}^{2+}$  ions based on illustration by Anderson et al., (2015)

### 3.2. Water Uptake Ability

The degree of water absorption by alginate/gauze dressings (FDA and CA) mimics the ability of dressings to absorb wound exudates (Saarai et al., 2012). Absorption of wound exudates is also an important parameter for cell attachment, as reported by the previous study (Sobhanian et al., 2019). A wound dressing that can swell helps to maintain a moist environment and protect the wound bed from possible infection from airborne transmission and drying (Oh et al., 2020).

Figure 8 shows the water absorption capacity of CA wound dressings after 1, 3, 7, 9, and 14 days of immersion in a wound exudate-like solution. From the results, the highest percentage of water absorbency was achieved on day 1 for 1% and 2% CA. As observed, the percentage of water uptake ability in 1% CA /gauze was slightly higher than in 2% CA /gauze. A loosely cross-linked alginate network of 1% CA /gauze dressing has greater water uptake than a 2% CA dressing because it allows water molecules to diffuse rapidly (Peng et al., 2012). Before this, both 1% and 2% CA/gauze dressings need to slowly degrade to

allow water molecules to penetrate. The degradation of the CA/gauze dressings is an ongoing process of ion exchange between  $\text{Ca}^{2+}$  ions bound to  $\text{COO}^-$  groups of the polymer and  $\text{Na}^+$  ions from the wound exudate solution, which consists of 8.298 g sodium chloride (NaCl) and 0.368 g calcium chloride dihydrate ( $\text{CaCl}_2 \cdot 2\text{H}_2\text{O}$ ) (Lencina et al., 2015). Then, the repulsion effects of the  $\text{COO}^-$  groups led to the loosening of the network chains (Lencina et al., 2015). The loosening of the network chains allowed more water molecules to penetrate and enhance the water absorption capacity of 1% CA/gauze dressings (Lencina et al., 2015).

In contrast, the ability of 2% CA/gauze dressing to absorb water decreased with decreasing porosity and showed a significant decrease on D7, 9 and 14. This happened due to more pores being formed at high concentrations of alginate (Saarai et al., 2012). This hinders the diffusion of water molecules into the gel as the structure of the pores becomes smaller (Saarai et al., 2012). Sikareepaisan et al. (2011) reported that the availability of binding sites for  $\text{Ca}^{2+}$  ions increases when the concentration of alginate increases. Therefore, the water absorption capacity of the 2% CA dressing is limited due to the larger cross-links and tighter gel networks formed between alginate and  $\text{Ca}^{2+}$  ions (Sikareepaisan et al., 2011). Therefore, the gelation process and the presence of a crosslinking agent contributed to the outcome of the results by controlling the movement of water molecules in the CA /gauze dressings.

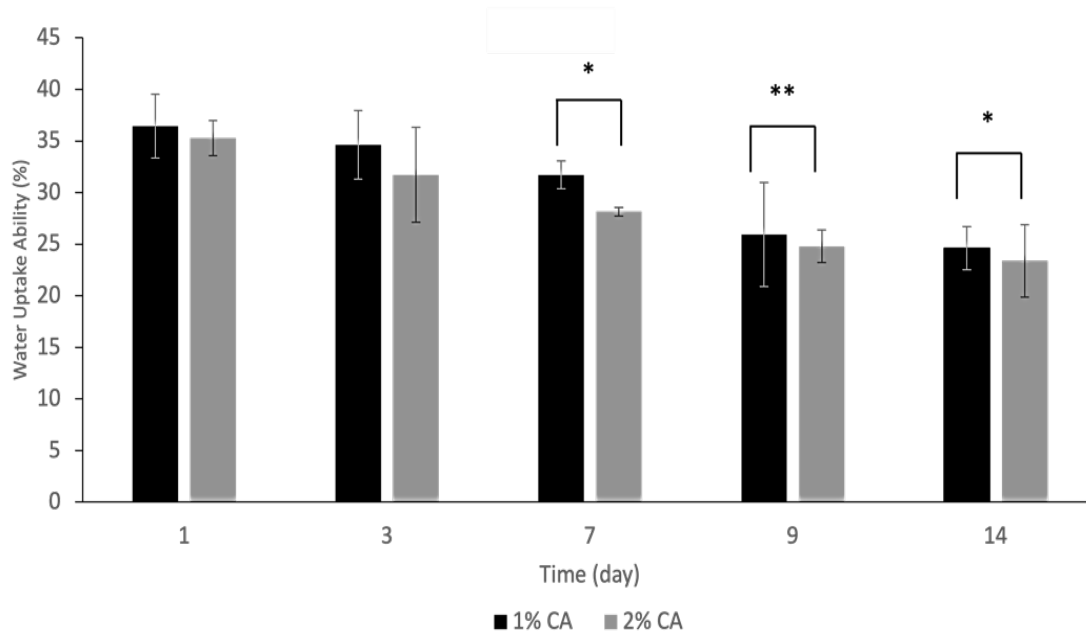


**Figure 8** Water Uptake Ability (%) of CA/gauze dressings for 14 days in wound exudate solution. Values are mean  $\pm$ SD from three replicates \*  $p < 0.05$ , \*\* $p < 0.01$

Based on a previous study, it was found that the water content and swelling capacity of sodium alginate increased with the increase of sodium alginate content (Kong et al., 2019). Similarly, another study observed that the swelling behaviour, release rate, and biodegradation of alginate increased when the amount of alginate was increased (He et al., 2015). The increased water absorption capacity of FDA/gauze dressings correlated with the hydrophilic nature of the alginate (Boateng and Catanzano, 2015). The presence of OH groups in alginate is attributed to the interactions of alginate with water molecules (He et al., 2015). However, an alginate-based spongy wound dressing, such as an FDA/gauze dressing, is suitable for treating wounds with large amounts of exudates (Sun & Tan, 2013). Therefore, FDA dressings have maximum capacity in absorbing wound fluids, especially in severe wounds with large amounts of exudates (Sun & Tan, 2013).

As shown in Figure 9, 2% FDA/gauze represents a significant value of water uptake ability from D1 to D14 when compared to 1% FDA/gauze. In contrast, CA/gauze dressings have an optimal water absorption capacity than FDA/gauze dressings due to the structural form of the dressings (Sun & Tan, 2013). On average, the percentage of FDA dressings is higher than that of CA dressings because the spongy shape of FDA/gauze enables it to absorb water maximally, unlike CA /gauze dressings, which consist of a gel-like structure that limits the ability to absorb more water (Sun & Tan, 2013). One study reported that the properties of alginate in terms of stability, elasticity, and water absorbency are also influenced by the presence and amount of the crosslinking agent used (Andersen et al., 2015). The large difference between the water absorbency of FDA/gauze and CA /gauze dressings was due to the crosslinking agent  $\text{CaCl}_2$ . The formation of networks in the form of an "egg box," which is formed by the binding of divalent cations such as  $\text{Ca}^{2+}$  ions to the G residues of the alginate, limited the diffusion of water molecules into the CA /gauze composites (Peng et al., 2012), whereas, in FDA/gauze composites, the crosslinking process between alginate and  $\text{Ca}^{2+}$  ions was absent and resulted in maximum water uptake.

In addition, Aderibigbe and Buyana (2018) found that the use of crosslinking agents in the preparation of alginate gel affects water absorption due to its high mechanical strength. In the absence of crosslinkers, FDA/gauze dressings manifest the hydrophilic nature of alginate to absorb large amounts of water as it is readily attracted to water molecules (Kong et al., 2019). Nevertheless, various types of alginate-based dressings can be used to treat wounds with moderate and heavy exudate, such as acute and chronic wounds (Peng et al., 2012).

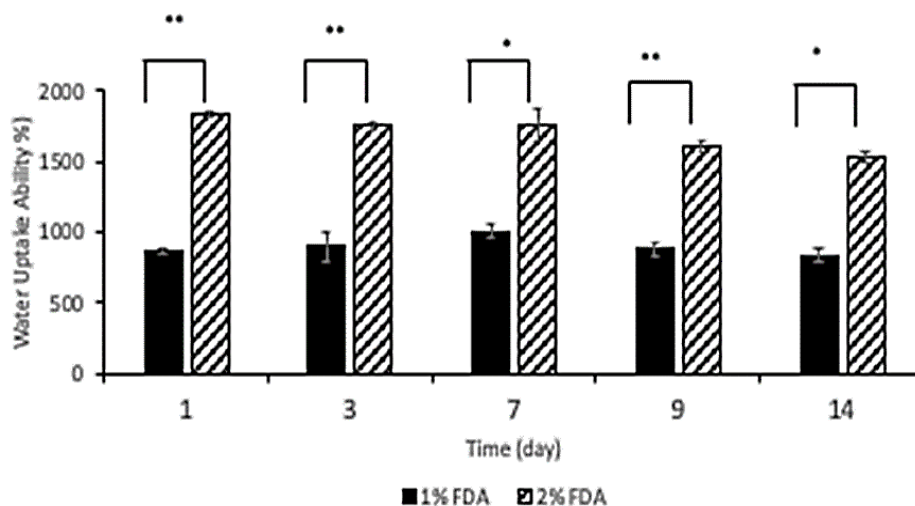


**Figure 9** Water Uptake Ability (%) of FDA/gauze dressings for 14 days in wound exudate solution. Values are mean  $\pm$ SD from three replicates \*  $p < 0.05$ , \*\* $p < 0.01$

### 3.2 Cell viability study

An ideal characteristic of wound dressings is mainly related to their ability to adhere to cells. This is because a good wound dressing provides a favourable environment for cell growth and proliferation (Sobhanian et al., 2019). Although a wound can be healed naturally through the regeneration of lost and damaged tissue, an appropriate wound dressing is required to mediate and promote the healing process (Sikareepaisan et al., 2011). According to Golafshan et al. (2017), alginate dressings in the form of gel and sponge are used as wound dressings because they can promote the cellular activities of the wound such as hemostasis, attachment, and proliferation of cells. In this study, the viable cells on FDA/gauze and CA /gauze dressings were observed under Nikon Eclipse inverted microscope (TS100).

Oh et al. (2020) studied that maintaining a moist environment around the wound site is crucial to promote fibroblast and keratinocyte migration and also to induce cell re-epithelialization. The preparation of CA dressings in the form of a gel is important to maintain a moist environment around the injured site (Peng et al., 2012). In addition, the moisture of the dressings is critical to stimulate the breakdown of fibrin and dead tissue, promoting angiogenesis, and increasing collagen synthesis (Oh et al., 2020). At the same time, CA dressings can absorb wound exudate in moderation to prevent wound dehydration. In addition, CA dressings support wound healing by providing water to dehydrated tissues while allowing the diffusion of oxygenated water vapour (Peng et al., 2012). Bagher et al. (2020) reported that the enlargement of pores during the swelling process is suitable for cell attachment and growth. Interestingly, FDA dressings undergo a gelling process during incubation in a wound exudate-like solution and form a gel structure. Therefore, both FDA and CA dressings have similar properties for supporting the growth of HSF cells. Nevertheless, FDA dressings are only suitable for wounds with heavy exudate (Sun & Tan, 2013). Therefore, a moist environment is beneficial as it accelerates the rate of wound healing and reduces pain and scarring (Oh et al., 2020).

Initially, the FDA/gauze and CA/gauze dressings were infused with extracts of HSL extract prior to the cell viability study, and the image of both samples is shown in Figure 10.  $1 \times 10^6$  HSF cells seeded on FDA/gauze and CA /gauze dressings. The amount of HSL extract used in the experiment is safe because it is below the IC<sub>50</sub>, which is 0.05 mg (Shadhan and Bohari, 2017). As can be seen in Figure 9 (1% FDA/gauze dressing) and Figure 10 (2% FDA/gauze dressing), the cells grew in the dressings. In addition, HSF cells were also observed on 1% and 2% CA /gauze dressings, as shown in Figures 11 and 12, respectively. The red circles on the photomicrographs represent the HSF cells.

HSL is known for its bioactive compounds such as flavonoids, polyphenols, and anthocyanins, which are used in folk medicine to treat diseases such as fever, liver disease, and hypertension (Malacrida et al., 2016). A study demonstrated the potential of ethanolic extracts of HSL as antibacterial agents against Gram-positive (*Staphylococcus aureus* and *Micrococcus luteus*) and Gram-negative bacteria (*Escherichia coli* and *Salmonella enteritidis*) (Borrás-Linares et al., 2015). In addition, Abdallah (2016) evaluated the antibacterial activities of methanolic extracts of HSL extract against Gram-positive (*S. aureus*, *Staphylococcus epidermidis*, and *Bacillus cereus*) and Gram-negative (*Pseudomonas aeruginosa*, *E. coli*, *Klebsiella pneumoniae*, *Salmonella enterica*, and *Proteus vulgaris*) bacteria compared to penicillin. The presence of some bioactive phytochemical constituents may be attributed to the antibacterial properties of HSL (Abdallah, 2016). Alshami & Alharbi (2014) suggested that the antimicrobial effects of HSL are likely exhibited by phenolic compounds through the formation of hydrogen bonds with certain vital proteins such as microbial enzymes or by iron deprivation. However, the antibacterial agent in HSL and its mechanism of action are yet to be understood (Abdallah, 2016).

In recent years, flavonoids are associated with the antimicrobial effects of HSL due to their ability to form a complex with the bacterial cell wall and affect cell wall permeability (Riaz & Chopra, 2018). There are a few possible mechanisms of action that take place, namely phosphorylation, inhibition of electron transport protein translocation, and enzyme-dependent reactions (Riaz & Chopra, 2018). As a result, the permeability of the plasma membrane increases and ion leakage from the bacterial cell occurs (Riaz & Chopra, 2018). Recently, Portillo-Torres et al. (2019) discovered that hibiscus acid from HSL

extracts is responsible for damaging the outer layer of the bacterial cell wall by directly affecting membrane permeability. The uptake of crystal violet dye into the bacterial cell was evidence that HSL successfully destroys *E. coli* and *Salmonella* when treated with hibiscus acid (Portillo-Torres et al., 2019).

After 24 hours of incubation, clumps of cells were detected on the dressings, which were HSF cells. This indicates that HSF cells can live and remain viable throughout incubation in the complete media on both FDA/gauze and CA/gauze dressings. The attachment of HSF cells confirms that the FDA and CA dressings promote cell growth. Based on a previous study by Shadhan and Bohari (2017), methanolic extracts of HSL and its fractions were shown to enhance wound healing activity *in vitro*. In this experiment, HSL extract was used as a potential therapeutic agent that plays an important role in wound healing. Therefore, the combination of alginate and HSL extract has high potential as a wound dressing, which needs to be investigated in detail for further use.

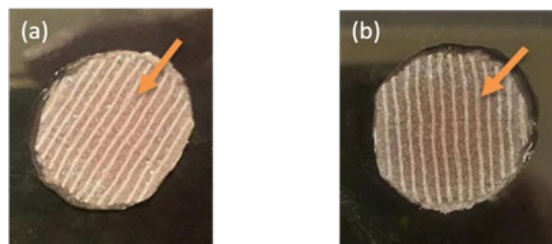


**Figure 10** Photographs of FDA/gauze and CA/gauze dressing infused with *Hibiscus sabdariffa* Linn.

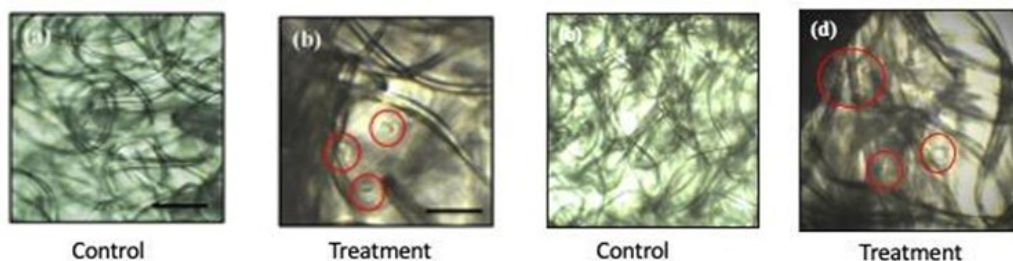


**Figure 11** Micrographs of freeze-dried alginate (FDA) dressing: 1% (a and b) and 2% (c and d) at 10x magnifications. Red circles represent the clump of HSF cells. Scale bar: 50  $\mu\text{m}$

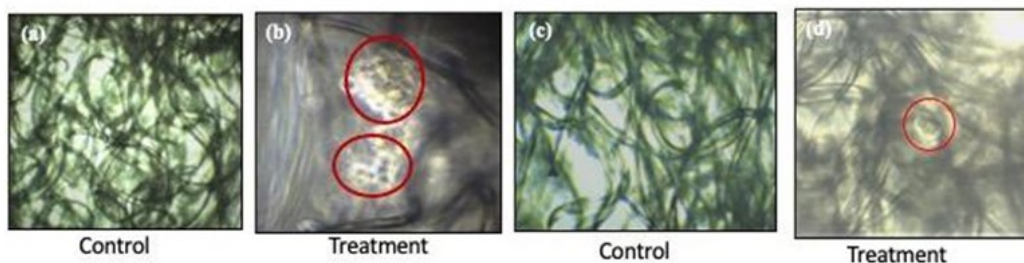


**Figure 12** Micrographs of calcium alginate (CA) dressings: 1% (a and b) and 2% (c and d) at 10x magnifications. Red circles represent the clump of HSF cells. Scale bar: 50  $\mu\text{m}$

#### 4.0 CONCLUSION

In conclusion, the preparation of alginate/gauze dressings (FDA/gauze and CA/gauze of two different forms (spongy and gel-like) and concentrations (1% and 2%) was successfully carried out by different procedures (freeze-drying and gelation). The presence of crosslinkers has a significant influence on the morphology of the dressings, with FDA/gauze dressings consisting of a porous structure, in contrast to CA/gauze dressings, which have a smooth surface. In addition, the physical structure of the dressings contributes to their ability to absorb water. Thus, FDA/gauze dressings have a higher water absorption capacity than CA/gauze dressings. The water absorption capacity increased with the concentration of alginate in FDA/gauze dressing. In contrast, the water-absorbing capacity of CA/gauze dressing decreased when the alginate concentration increased because more binding sites for  $\text{Ca}^{2+}$  ions were available. The ability of an alginate/gauze dressing to absorb water is critical for providing moist conditions for the wounded area. In addition, the incorporation of HSL extract in alginate/gauze dressings showed beneficial effects on HSF cells by maintaining viability and proliferation for a longer period. Therefore, extensive research needs to be conducted to evaluate the therapeutic benefits of HSL for wound healing in order to use it as a potential agent in wound dressings.



## Acknowledgement

This work was funded by the Ministry of Education (MOE) through Fundamental Research Grant Scheme (FRGS/1/2020/STG01/UTM/02/8).

## References

- Abdallah, E. M. (2016). Antibacterial efficiency of the Sudanese Roselle (*Hibiscus sabdariffa* L.), a famous beverage from Sudanese folk medicine. *Journal of Intercultural Ethnopharmacology*. 5(2), 186.
- Aderibigbe, B. A., & Buyana, B. (2018). Alginate in wound dressings. *Pharmaceutics*. 10(2), 42.
- Alshami, I., & Alharbi, A. E. (2014). *Hibiscus sabdariffa* extract inhibits in vitro biofilm formation capacity of *Candida albicans* isolated from recurrent urinary tract infections. *Asian Pacific Journal of Tropical Biomedicine*. 4(2), 104-108.
- Andersen, T., Auk-Emblem, P., & Dornish, M. (2015). 3D Cell Culture in Alginate Hydrogels. *Microarrays (Basel)*. 4(2), 133-161.
- Bagher, Z., Ehterami, A., Safdel, M. H., Khastar, H., Semiari, H., Asefnejad, A., Davachi, S. M., Mirzaii, M. and Salehi, M. (2020). Wound healing with alginate/chitosan hydrogel containing hesperidin in rat model. *Journal of Drug Delivery Science and Technology*. 55, 101379.
- Bahadoran, M., Shamloo, A., & Nokoorani, Y. D. (2020). Development of a polyvinyl alcohol/sodium alginate hydrogel-based scaffold incorporating bFGF-encapsulated microspheres for accelerated wound healing. *Scientific Reports*. 10(1), 1-18.
- Bhardwaj, N., Chouhan, D., & Mandal, B. B. (2018). 3D functional scaffolds for skin tissue engineering. in *Functional 3D tissue engineering scaffolds* (pp. 345-365). Woodhead Publishing.
- Bohari, S. P., Hukins, D. W., & Grover, L. M. (2011). Effect of calcium alginate concentration on viability and proliferation of encapsulated fibroblasts. *Bio-Medical Materials and Engineering*, 21(3), 159-170.
- Borrás-Linares, I., Fernández-Arroyo, S., Arráez-Roman, D., Palmeros-Suárez, P. A., Del Val-Díaz, R., Andrade-González, I., Fernández-Gutiérrez, A., Gómez-Leyva, J. F. and Segura-Carretero, A. (2015). Characterization of phenolic compounds, anthocyanidin, antioxidant and antimicrobial activity of 25 varieties of Mexican Roselle (*Hibiscus sabdariffa*). *Industrial Crops and Products*. 69, 385-394.
- Catanzano, O., D'esposito, V., Acierno, S., Ambrosio, M.R., De Caro, C., Avagliano, C., Russo, P., Russo, R., Miro, A., Ungaro, F. and Calignano, A. (2015). Alginate-hyaluronan composite hydrogels accelerate wound healing process. *Carbohydrate polymers*. 131, 407-414.
- Chen, H., Xing, X., Tan, H., Jia, Y., Zhou, T., Chen, Y., Ling, Z. and Hu, X. (2017). Covalently antibacterial alginate-chitosan hydrogel dressing integrated gelatin microspheres containing tetracycline hydrochloride for wound healing. *Materials Science and Engineering: C*. 70, 287-295.
- Golafshan, N., Rezasahani, R., Esfahani, M. T., Kharaziha, M., & Khorasani, S. (2017). Nanohybrid hydrogels of laponite: PVA-Alginate as a potential wound healing material. *Carbohydrate Polymers*. 176, 392-401.
- He, Y., Wu, Z., Tu, L., Han, Y., Zhang, G., & Li, C. (2015). Encapsulation and characterization of slow-release microbial fertilizer from the composites of bentonite and alginate. *Applied Clay Science*. 109, 68-75.
- Kamoun, E. A., Kenawy, E.-R. S., & Chen, X. (2017). A review on polymeric hydrogel membranes for wound dressing applications: PVA-based hydrogel dressings. *Journal of Advanced Research*, 8(3), 217-233.
- Kong, F., Fan, C., Yang, Y., Lee, B. H., & Wei, K. (2019). 5-hydroxymethylfurfural-embedded poly (vinyl alcohol)/sodium alginate hybrid hydrogels accelerate wound healing. *International Journal of Biological Macromolecules*. 138, 933-949.
- Lencina, M. S., Ciolino, A. E., Andreucetti, N. A., & Villar, M. A. (2015). Thermoresponsive hydrogels based on alginate-g-poly (N-isopropylacrylamide) copolymers obtained by low doses of gamma radiation. *European Polymer Journal*. 68, 641-649.
- Malacrida, A., Maggioni, D., Cassetti, A., Nicolini, G., Cavaletti, G., & Miloso, M. (2016). Antitumoral effect of *Hibiscus sabdariffa* on human squamous cell carcinoma and multiple myeloma cells. *Nutrition and cancer*. 68(7), 1161-1170.
- Mohandas, A., Sudheesh Kumar, P., Raja, B., Lakshmanan, V.-K., & Jayakumar, R. (2015). Exploration of alginate hydrogel/nano zinc oxide composite bandages for infected wounds. *International journal of nanomedicine*. 10(Suppl 1), 53.
- Montanucci, P., Terenzi, S., Santi, C., Pennoni, I., Bini, V., Pescara, T., Basta, G. and Calafiore, R. (2015). Insights in behavior of variably formulated alginate-based microcapsules for cell transplantation. *BioMed Research International*. 2015.
- Oh, G.-W., Nam, S. Y., Heo, S.-J., Kang, D.-H., & Jung, W.-K. (2020). Characterization of ionic cross-linked composite foams with different blend ratios of alginate/pectin on the synergistic effects for wound dressing application. *International Journal of Biological Macromolecules*. 156, 1565-1573.
- Peng, C.-W., Lin, H.-Y., Wang, H.-W., & Wu, W.-W. (2012). The influence of operating parameters on the drug release and antibacterial performances of alginate wound dressings prepared by three-dimensional plotting. *Materials Science and Engineering: C*. 32(8), 2491-2500.
- Portillo-Torres, L.A., Bernardino-Nicanor, A., Gómez-Aldapa, C.A., González-Montiel, S., Rangel-Vargas, E., Villagómez-Ibarra, J.R., González-Cruz, L., Cortés-López, H. and Castro-Rosas, J. (2019). Hibiscus acid and chromatographic fractions from *Hibiscus sabdariffa* calyces: Antimicrobial activity against multidrug-resistant pathogenic bacteria. *Antibiotics*. 8(4), 218.
- Riaz, G., & Chopra, R. (2018). A review on phytochemistry and therapeutic uses of *Hibiscus sabdariffa* L. *Biomedicine & Pharmacotherapy*. 102, 575-586.
- Saarai, A., Sedlacek, T., Kasparkova, V., Kitano, T., & Saha, P. (2012). On the characterization of sodium alginate/gelatine-based hydrogels for wound dressing. *Journal of Applied Polymer Science*. 126(S1), E79-E88.

- Shadhan, R. M., & Bohari, S. P. M. Effects of *Hibiscus sabdariffa* Linn. fruit extracts on  $\alpha$ -glucosidase enzyme, glucose diffusion and wound healing activities. Cell. 19, 20.
- Sikareepaisan, P., Ruktanonchai, U., & Supaphol, P. (2011). Preparation and characterization of asiaticoside-loaded alginate films and their potential for use as effectual wound dressings. Carbohydrate Polymers. 83(4), 1457-1469.
- Sobhanian, P., Khorram, M., Hashemi, S. S., & Mohammadi, A. (2019). Development of nanofibrous collagen-grafted poly (vinyl alcohol)/gelatin/alginate scaffolds as potential skin substitute. International Journal of Biological Macromolecules, 130, 977-987.
- Summa, M., Russo, D., Penna, I., Margaroli, N., Bayer, I.S., Bandiera, T., Athanassiou, A. and Bertorelli, R. (2018). A biocompatible sodium alginate/povidone iodine film enhances wound healing. European Journal of Pharmaceutics and Biopharmaceutics, 122, 17-24.
- Sun, J., & Tan, H. (2013). Alginate-based biomaterials for regenerative medicine applications. Materials, 6(4), 1285-1309.
- Wan, Y., Chen, X., Xiong, G., Guo, R., & Luo, H. (2014). Synthesis and characterization of three-dimensional porous graphene oxide/sodium alginate scaffolds with enhanced mechanical properties. Materials Express. 4(5), 429-434.